Results in Materials 9 (2021) 100168

Contents lists available at ScienceDirect

Results in Materials

journal homepage: www.journals.elsevier.com/results-in-materials

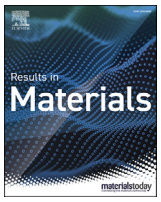

Comparative study of textile material characterization techniques for wearable antennas

Jeremiah O. Abolade [a,*], Dominic B.O. Konditi [b], Vasant M. Dharmadhikary [c]

[a] Department of Electrical Engineering, Pan African University, Institute for Basic Sciences, Technology and Innovation, Nairobi, Kenya
[b] School of Electrical and Electronic Engineering, The Technical University of Kenya, Nairobi, Kenya
[c] Department of Electrical and Electronic Engineering, Dedan Kimathi University of Technology, Nyeri, Kenya

ARTICLE INFO

Keywords:
Textile material
Stub resonator
Ring resonator
Aso-Oke
Wearable antenna

ABSTRACT

A comparative study of Quarter-wavelength λ4 stub and ring resonator techniques for the characterization of four (4) different textile materials (*Kente-Oke* (M1), *Sanya* (M2), *Alaari* (M3) and *Etu* (M4)) are presented in this work for the first time. The materials characterized in this work are locally made handwoven textile called "Aso-Oke" in South-west, Nigeria. The simulation and measurement results are presented. The dielectric parameters of materials were found to be 1.68, 1.46, 1.32, 1.51 for M1, M2, M3, and M4 respectively, and corresponding loss tangent of 0.049, 0.061, 0.019, 0.059 using Ring resonator. In the same light, the permittivity of the material M1, M2, M3, and M4 are found to be 1.75, 1.75, 1.5, 1.5 respectively, and corresponding loss tangent of 0.5, 0.6, 0.2, 0.6 using Quarter-wavelength open end Stub resonator. Using the parameters extracted from characterization, the materials are used as the substrate for wearable antenna to validate the measured dielectric properties of the material under test (MUTs). The results of this work show that, stub technique is more accurate than the ring resonator techniques. This is because of the complexity of ring resonator technique which makes it prone to fabrication error compared to the simplicity of the stub resonator technique. However, stub resonator technique can be time consuming due to the manual adjustment of the relative permittivity of the material during simulation. It is observed from the results of this research that, the stub resonator results are comparable to the Ring resonator-based results. Hence, combining the two techniques by using the ring resonator to predict the region of the relative permittivity and then using the stub resonator technique to optimize the accuracy by varying the permittivity around the predicted region provided by ring resonator technique shall reduce the time consumed by Stub-resonator and increases the accuracy of the measurement.

1. Introduction

Wearable devices have become part of human life [1]. They are primarily worn either on the body called On-body application or placed inside the body called In-body application [2]. These devices are usually built as part of wearable material such as clothes, wristwatch, shoes and so on. A wearable device should be of lightweight, conformal, not harmful to human tissues [3]. Wearable antennas are antennas that are suitable for wearing either on-body or in-body [4,5]. Textile materials could be conductive or non-conductive. The non-conductive textiles are usually used as the substrates of wearable antennas to reduce the weight and the profile of the antenna when compared with the standard substrates [6]. Antennas' profile is generally dependent on the permittivity, thickness and loss tangent of the substrate used [7].

Therefore, before any textile can be used for wearables, it must be characterized to extract these parameters (relative permittivity, thickness, and loss tangent) [6–10]. Several techniques have been proposed by the authors in the literature such as, Coaxial Probe technique [11–14], Split-ring resonator technique [15], complementary split-ring resonator [16], ring-resonator [6,17], quarter-wave open end stub resonator among others.

Among these techniques, ring-resonator technique and quarter-wave open end stub resonator technique are commonly used due to their ease of fabrication and low cost of measurement [[15–18]]. They are categorized under resonator-based material characterization techniques. Even though these are commonly used by researchers, comparative study of these two techniques has not been performed in the literature. Hence, this work focuses on the comparative analysis of the two techniques.

* Corresponding author.
E-mail address: aboladejeremiah@yahoo.com (J.O. Abolade).

https://doi.org/10.1016/j.rinma.2021.100168
Received in revised form 7 January 2021; Accepted 10 January 2021
Available online 23 January 2021

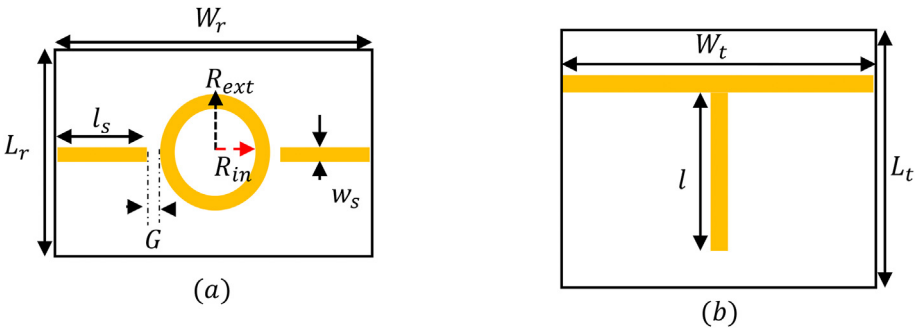

Fig. 1. The configuration of the: (a) Ring resonator (b) Quarter-wavelength open end stub.

Table 1
The design parameters of the ring and stub resonators.

Parameter	Wr	ws	Lr	ls	Rext	Rin	G	Wt	Lt	l
Value (mm)	50	3	50	14	10	7	1	53	53	26.5

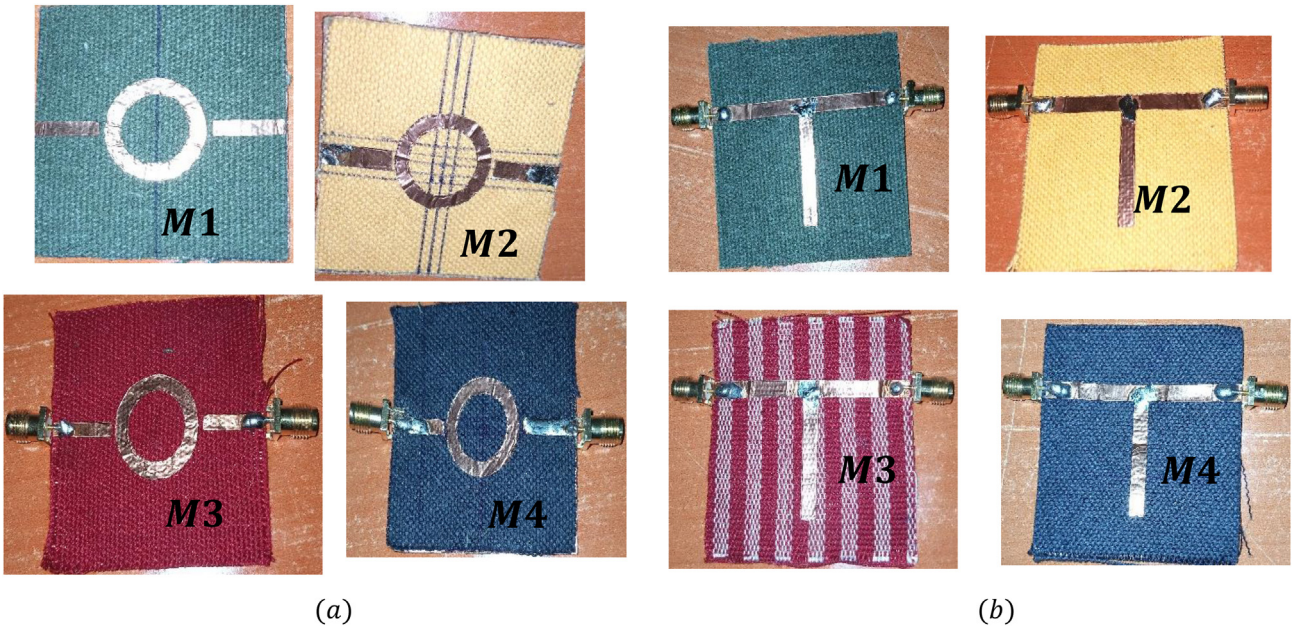

Fig. 2. Implementation of (a) Ring resonator and (b) Stub resonator on M1, M2, M3, and M4.

Aso-Oke are locally made handwoven fabric which originated from the southwestern region of Nigeria. They are made locally by weaving and are made of different thickness and material such as cotton, flax, fiber and wax [19]. These materials are generally being used for coverings due to its durability, reliability and thickness. It was commonly worn by the aged people in the southwestern region of Nigeria in the 50s. Kente-Oke (M1) is made from silk, wax and cotton. *Anaphe* wild silk along with cotton yarns are used in woven Sanya (M2); locally spurned silk yarn Alaari (M3) and the Etu textile material (M4) is woven from a locally grown wild silk fibre [20]. The spurning thickness of silk fibre is a major distinction among the material under test. The detail process of the making of these materials is provided by the authors in Ref. [19].

Though, these materials (Aso-Oke) started locally, it has become a global textile material. As part of the contribution of this work, the electrical and electromagnetic characterization of Aso-Oke is presented in this work for the first time.

2. The design of ring and stub resonators for textile characterization

The ring resonator and the λ4 stub resonator is presented in Fig. 1a and b respectively. The values of the parameters in Fig. 1a and b are given in Table 1.

Wr and Lr are the width and length of the ring resonator substrate respectively, ws and ls are the width and the length of the ring resonator feedline respectively, Rext and Rin are the radius of the outer circle and the inner circle respectively, G is the width of the gap between the microstrip feedline and the ring, Wt and Lt are the width and length of the quarter-wavelength resonator substrate respectively, and l is the length of the stub which is λ4. Fig. 1a and b are replicated in on the textile materials for characterization as shown in Fig. 2a and b respectively on each of the materials. The material used are all plain-woven material (Aso-Oke) with different texture. The Green, yellow, Wine and Blue colors are called *Kente-Oke* (M1), *Sanya* (M2), *Alaari* (M3) and *Etu* (M4) respectively.

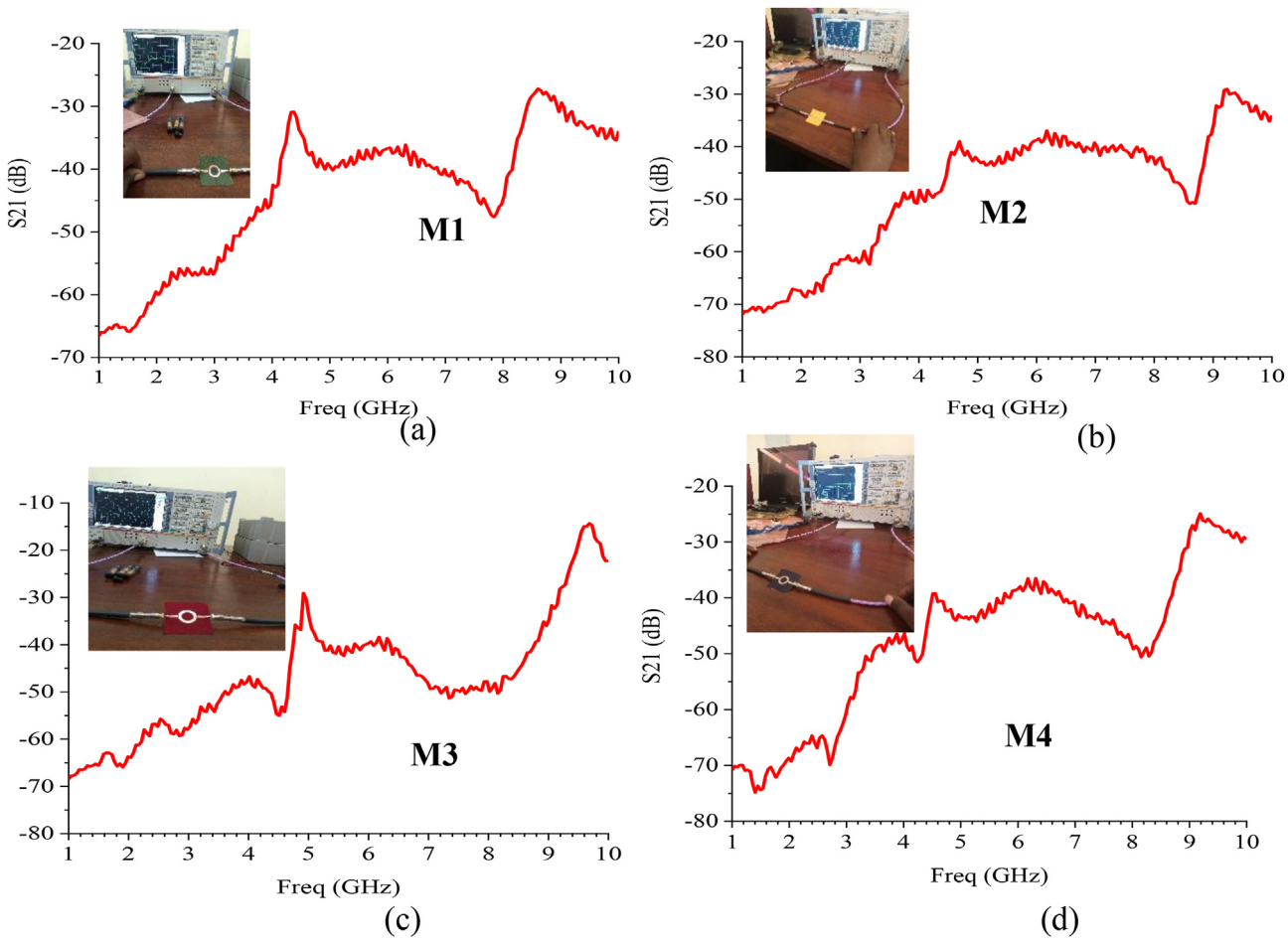

Fig. 3. The S21 of the MUT using Ring resonator technique.

Table 2
Ring Resonator Technique for wearable material Characterization.

Material	n	f_o (GHz)	S_{21} (dB)	-3dB (BW)		εr	tanδ	Average ε_r	Average
				tanδ	f_l				
M1	1	4.35	−30.86	4.27	4.46	1.67	0.041	1.68	0.049
	2	8.61	−27.22	8.42	8.94	1.70	0.057		
M2	1	4.69	−39.15	4.52	4.88	1.43	0.074	1.46	0.061
	2	9.22	−29.14	9.15	9.62	1.48	0.048		
M3	1	4.92	−29.20	4.89	4.99	1.30	0.018	1.32	0.019
	2	9.69	−14.40	9.52	9.77	1.34	0.02		
M4	1	4.53	−39.22	4.45	4.47	1.54	0.062	1.51	0.059
	2	9.19	−24.91	9.02	9.58	1.49	0.056		

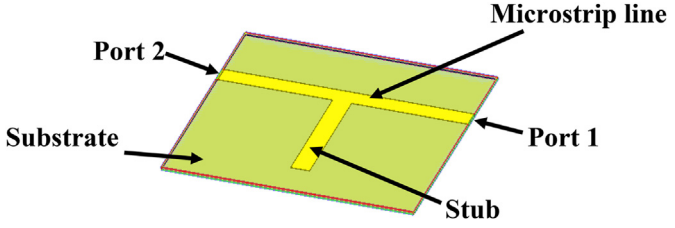

Fig. 4. Simulation configuration of the quarter-wavelength open end stub resonator.

Table 3
$\frac{\lambda}{4}$ open end stub Resonator Technique for wearable material Characterization.

Material	Measurement		Optimized Parameters		Simulation	
	f_o (GHz)	S_{21} (dB)	ε_r	tanδ	f_o (GHz)	S_{21} (dB)
M1	2.15	−23.24	1.75	0.05	2.15	−19.56
M2	2.17	−21.40	1.75	0.06	2.17	−18.20
M3	2.36	−38.93	1.5	0.02	2.36	−26.71
M4	2.26	−23.18	1.5	0.06	2.32	−18.94

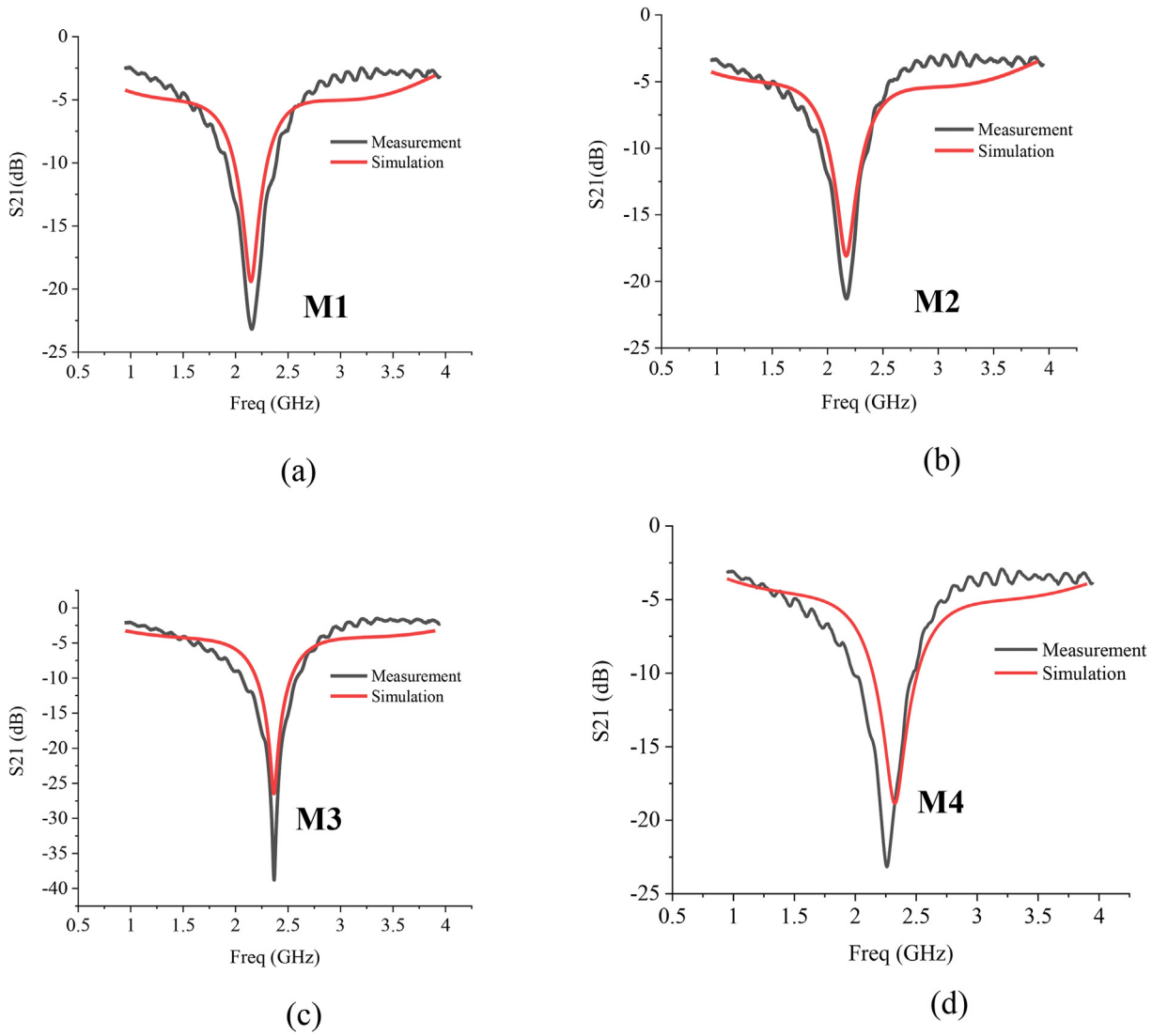

Fig. 5. The measurement and simulation S21 of the stub resonator.

The thickness of M1, M2, M3 and M4 are 0.8 mm, 0.5 mm, 0.7 mm, and 0.6 mm respectively. The thickness of the adhesive copper used in this work is 80 μm.

The design of the ring resonator is based on the modelling equation [17] presented in Eqns. (1)–(6)

$$f_n = \frac{nC_o}{2\pi R_m \sqrt{\varepsilon_r}} \tag{1}$$

where fn is the band-stop (Peak value of S_{21}) frequency of nth mode, Rm is the average of the sum of Rext and Rin and it is referred to as mean radius, Co is the free space velocity (3×10^8 m/s), and ε_r is the relative permittivity of the material under test (MUT).

It is clear that, ε_r can be determined from Eqn. (1), once the transmission coefficient (S_{21}) at the nth mode of the ring is known through measurement.

The loss tangent of the material can be calculated using Eqn. (2) [6].

$$\tan\delta = \frac{1}{Q_d} \tag{2}$$

where Q_d is the quality factor of the dielectric. In order to determine Q_d, the unloaded quality factor must be determined. These two are related as shown in Eqn. (3)

$$\frac{1}{Q_u} = \frac{1}{Q_d} + \frac{1}{Q_c} \tag{3}$$

where Qu is the unloaded quality factor, and Qc stands for the quality factor due to conduction which is determined by using Eqn. (4)

$$Q_c = h(f_o \mu_o \pi \sigma_c)^{0.5} \tag{4}$$

where fo is the resonance frequency, μ_o and σ_c are free space permeability and conductivity of copper respectively.

In other to determine Q_u the insertion loss (S_{21} dB) formula [21] is recalled and given in Eqn. (5)

$$IL = 20\log\left(1 - \frac{Q_L}{Q_u}\right) \tag{5}$$

where Q_L is the loaded quality factor and it can be determined by using Eqn. (6)

$$Q = \frac{f_o}{f_h - f_l} \tag{6}$$

where f_h and f_l are the upper and the lower frequencies at 3 dB around f_o.

Therefore, from Eqn. (5), Q_u can be determined. Hence, loss tangent (tanδ) can be calculated through Eqn. (2).

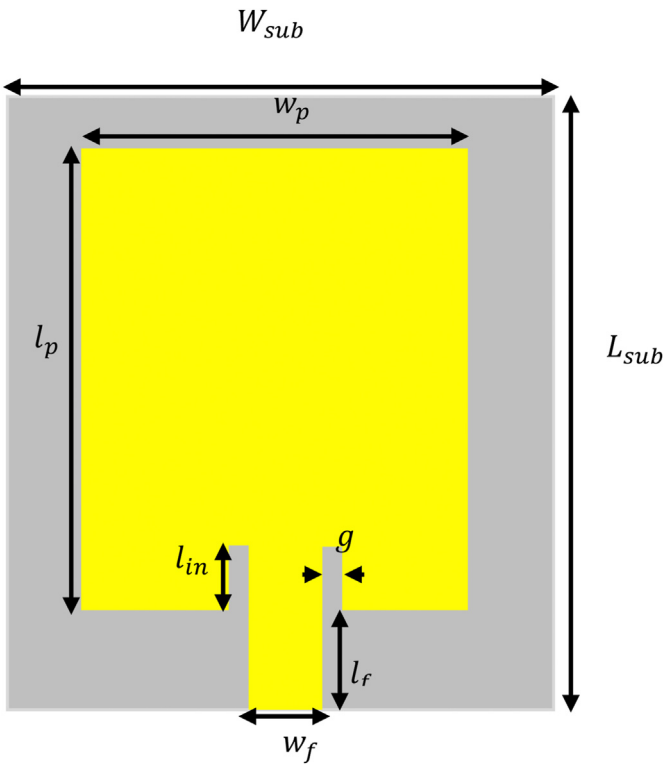

Fig. 6. The configuration of a wearable rectangular patch antenna.

Table 4
The dimension of the wearable patch antenna.

Parameters	W_{sub}	w_f	w_p	L_{sub}	l_f	l_p	l_{in}	g
Values (mm)	50	3	30	65	10	45	5	1

For quarter-wavelength open stub resonator technique, the length of the stub is designed to be λ_4 That is,

$$l = \frac{\lambda}{4} \tag{7}$$

Where λ is the wavelength in meter (m). The microstrip line is designed to be 2l i.e. half-wavelength. The transmission coefficient (S_{21} (dB)) is extracted from measurement and the same configuration is simulated with a substrate of an arbitrary permittivity using HFSS®. The value of the permittivity is then varied to achieve a simulation S_{21} that is close to the measured S_{21}.

3. Results and discussion

3.1. εr and tanδ using ring resonator technique

The measured transmission coefficient (S_{21}) of the material M1, M2, M3, and M4 using R&S ZVA 50 VNA are presented in Fig. 3a, b, c and d respectively. The adhesive copper tape of a 0.08 mm thickness is used for the resonators and the ground plane. It can be observed from Fig. 3 that the all the material has two distinct peaks each. The extracted parameters from Fig. 3 and the calculated εr and tanδ using Eqns. (1)–(6) are presented in Table 2.

It can be seen from Table 2 that Material M1 has the highest permittivity with relatively lowf_h tan δ. It is worthy of note also that material M3 has the lowest permittivity as well as the tan δ. Material M2 and M4 are approximately the same in both permittivity and loss tangent. With these properties, material M1 is suitable for compact wearable antenna due to its high permittivity and thickness, but when gain and radiation efficiency are of importance, material M3 is more suitable because of its thinness and low tan δ.

3.2. ε_r and tanδ using quarter-wavelength stub resonator technique

The configuration presented in Fig. 2b are connected to the VNA and S_{21} for each of the materials are extracted. Then, the same configuration is designed in HFSS® for each of the material as shown in Fig. 4.

After several variations of the permittivity of the simulation substrate, the permittivity of each of the materials are presented in Table 3 and the results of the transmission coefficient for both measurement and simulation for material M1, M2, M3, and M4 are presented in Fig. 5 a, b, c, and d respectively.

It can be observed that with the permittivity of M1 and M2 equal to 1.75, and that of M3 and M4 equal 1.5, the results of simulation agree well with the measurement results. It can be observed from Fig. 5 that the measured S21 are generally low compared with the simulation result. This could be due to the boundary conditions imposed during simulation. It is worthy of note that the permittivity and loss tangent of the material M1, M2, M3 and M4 by using the stub resonator technique are comparable to the values from the Ring resonator technique.

4. The design of a wearable antenna for validation

In order to validate our characterization, the same configuration of a rectangular patch wearable antenna has been simulated, and fabricated using each of the materials presented in the previous section. The structure of the wearable antenna is as shown in Fig. 6 and its dimensions

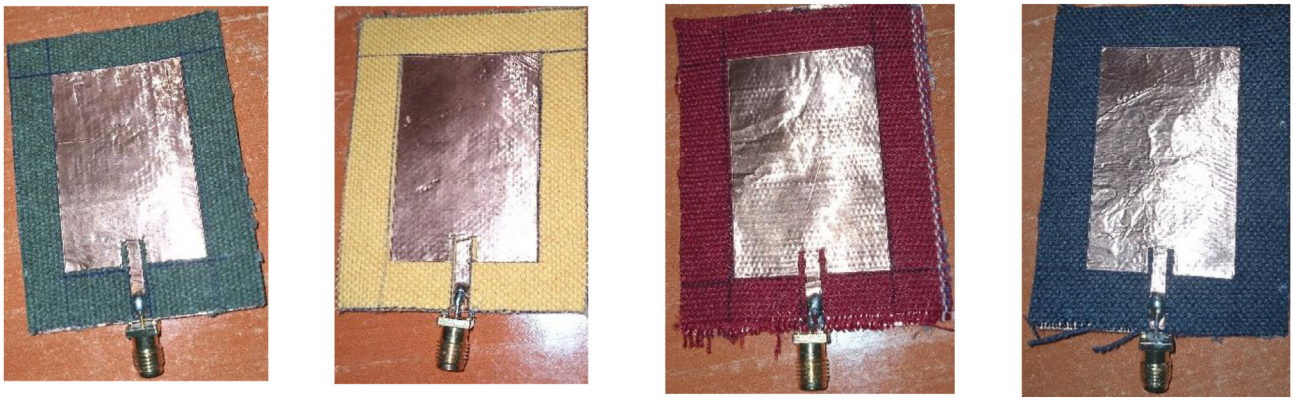

Fig. 7. The fabricated wearable antenna on material (a) M1, (b) M2, (c) M3 and (d) M4.

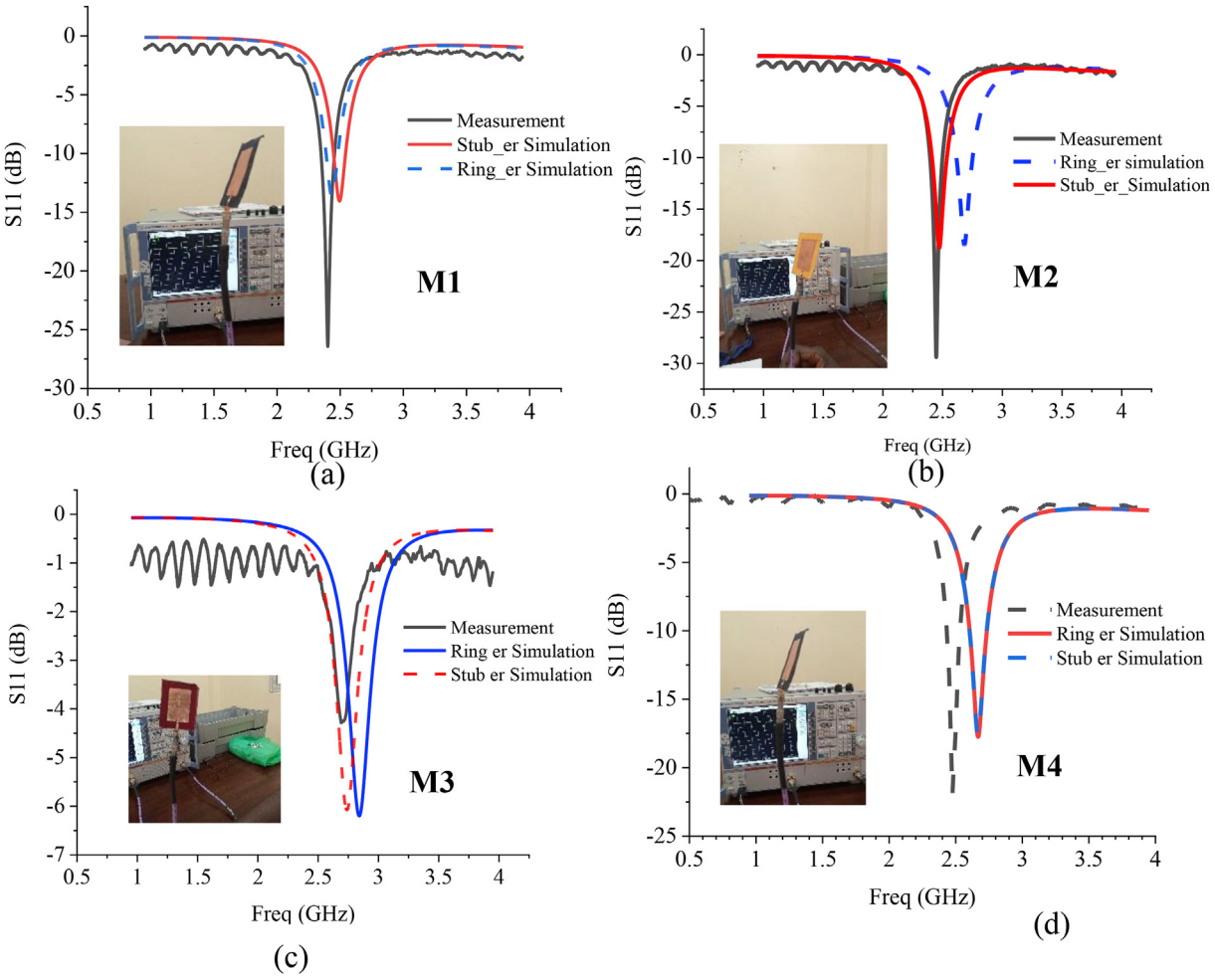

Fig. 8. The comparative S11 results of the measurement, stub-based simulation and Ring-based simulation.

Table 5
The Resonant frequency and the corresponding S11 of the wearable antenna using MUT.

Antenna Substrate	M1		M2		M3		M4	
Parameter	Freq (GHz)	S_{11} (dB)	Freq (GHz)	S_{11} (dB)	Freq (GHz)	S_{11} (dB)	Freq (GHz)	S_{11} (dB)
Measurment	2.41	−26.58	2.44	−29.336	2.71	−4.23	2.48	−21.79
Ring ε_r	2.42	−13.31	2.69	−18.67	2.84	−6.11	2.68	−17.75
Stub ε_r	2.49	−14.03	2.46	−19.06	2.73	−6.09	2.65	−17.55

are given in Table 4.

The configuration proposed in Fig. 6 is fabricated on all the MUT to verify the characteristic parameters presented in the previous section.

Fig. 7a, b, c, and d are the fabrications of the proposed structure on M1, M2, M3, and M4 respectively. It should be noted that a full ground plane is used in this work.

The measurement results and Simulation results using materials' properties given by the ring resonator (presented in Table 2) as well as stub resonator (given in Table 3) are presented in Fig. 8a, b, c and d for material M1, M2, M3 and M4 respectively.

It can be observed from Fig. 8 that the simulation results agree with the measurement results. Notwithstanding, the simulation result of Stub-based parameters are more in agreement with the measurement than that of Ring resonator based parameters as shown in Table 5. This can be traced to the complexity of the ring resonator which required extraordinary carefulness to minimize the fabrication error [16]. Though, Stub-based is simple, but it is time consuming to actually get the exact permitivity of the MUT. This is because after measuring the S_{21}, the entire simulation is based on trial and error. Therefore, seeing that, from the result herein presented, the stub-based material characteristics are in the neighborhood of that of Ring resonator based, the ring resonator can be used to determine the neighborhood of the textile permittivity and then use the stub resonator technique to tune the permitivity to the actual value. This will minimize the time consumption of the stub resonator technique and enhances the accuracy of the material characterization.

5. Conclusion

A comparative analysis of the two commonly used textile characterization techniques is presented for the first time. It has been demonstrated that the two techniques are suitable for material characterization. Even though stub resonator demonstrated higher accuracy, its adjustment is time consuming. Based on the results of this analysis, the hybridization of the two techniques has been proposed for time management and accuracy. The characterization of four (4) new hand-woven textile materials in the group of *Aso-Oke,* (a locally made textile in

Southwestern region, Nigeria, West Africa) is another contribution of this work to the existing literature. The prototype antenna fabrication and measurement have shown that the extracted characteristics of the Aso-Oke are accurate and can be used to design wearable antennas for medical and remote sensing applications among others.

Author statement

Jeremiah O. ABOLADE, Contributions include conception, design, Measurement, Result analysis, Preparation and revision of the manuscript. Dominic B. O. KONDITI, Contributions include analysis, Preparation and revision of the manuscript. Vasant M. DHARMADHIKARY, Contributed in preparation and revision of the manuscript.

Data availability

The data supporting the findings of this study are all presented within the article.

Declaration of competing interest

The authors declare that they have no known competing financial interests or personal relationships that could have appeared to influence the work reported in this paper.

Acknowledgments

This work was sponsored and supported by the African Union through the Pan African University Institute of Basic Sciences, Technology, and Innovation.

References

[1] A. Bonfiglio, D. De Rossi, Wearable Monitoring Systems, first ed., Springer, New York, NY, USA, 2011.
[2] B. Moradi, R. Fernández-García, I. Gil, Wearable high-performance meander ring dipole antenna for electronic-textile applications, J. Text. Inst. 111 (2) (2020) 178–182, https://doi.org/10.1080/00405000.2019.1628886.
[3] A.Y.I. Ashyap, et al., Compact and low-profile textile EBG-based antenna for wearable medical applications, IEEE Antenn. Wireless Propag. Lett. 16 (2017) 2550–2553, https://doi.org/10.1109/LAWP.2017.2732355.
[4] P. Salonen, Y. Rahmat-Samii, M. Schaffrath, M. Kivikoski, Effect of textile materials on wearable antenna performance: a case study of GPS antennas, in *IEEE Antennas and Propagation Society Symposium* 1 (2004) 459–462, https://doi.org/10.1109/APS.2004.1329673.
[5] R. Salvado, C. Loss, R. Gonçalves, P. Pinho, Textile materials for the design of wearable antennas: a survey, Sensors 12 (11) (2012) 15841–15857, https://doi.org/10.3390/s121115841.
[6] M.I. Ahmed, M.F. Ahmed, A.A. Shaalan, Investigation and comparison of 2.4 GHz wearable antennas on three textile substrates and its performance characteristics, Open J. Antenn. Propag. 5 (3) (2017) 110–120, https://doi.org/10.4236/ojapr.2017.53009.
[7] D. Ferreira, P. Pires, R. Rodrigues, R.F.S. Caldeirinha, Wearable Textile Antennas: examining the effect of bending on their performance, IEEE Antenn. Propag. Mag. 59 (3) (2017) 54–59, https://doi.org/10.1109/MAP.2017.2686093.
[8] D. Ram Sandeep, N. Prabakaran, B.T.P. Madhav, K.L. Narayana, P. Rakesh Kumar, Systematic investigation from material characterization to modeling of jute-substrate-based conformal circularly polarized wearable antenna, J. Electron. Mater. 49 (12) (2020) 7292–7307, https://doi.org/10.1007/s11664-020-08536-6.
[9] J. Lacik, et al., Characterization of 3D-knitted substrates, in: In *2020 23rd International Microwave And Radar Conference*, MIKON, 2020, pp. 241–243, https://doi.org/10.23919/MIKON48703.2020.9253876.
[10] A. Carnevale, et al., Conductive textile element embedded in a wearable device for joint motion monitoring, in: In *2020 IEEE International Symposium On Medical Measurements And Applications*, MeMeA, 2020, pp. 1–6, https://doi.org/10.1109/MeMeA49120.2020.9137251.
[11] S.A. Komarov, A.S. Komarov, D.G. Barber, M.J.L. Lemes, S. Rysgaard, Open-Ended coaxial probe technique for dielectric spectroscopy of artificially grown sea ice, IEEE Trans. Geosci. Rem. Sens. 54 (8) (2016) 4941–4951, https://doi.org/10.1109/TGRS.2016.2553110.
[12] M. Wu, X. Yao, L. Zhang, An improved coaxial probe technique for measuring microwave permittivity of thin dielectric materials, Meas. Sci. Technol. 11 (11) (2000) 1617–1622, https://doi.org/10.1088/0957-0233/11/11/311.
[13] J.C. Santos, M. Dias, A. Aguiar, I. Jr, L. Borges, Using the coaxial probe method for permittivity measurements of liquids at high temperatures, J. Microwaves, Optoelectron. Electromagn. Appl. 8 (2009) 78S–91S.
[14] V. Guihard, F. Taillade, J. Balayssac, B. Steck, J. Sanahuja, F. Deby, Permittivity measurement of cementitious materials with an open-ended coaxial probe, Construct. Build. Mater. 230 (Jan) (2020), https://doi.org/10.1016/j.conbuildmat.2019.116946.
[15] R. Hopkins, C. Free, Equivalent circuit for the microstrip ring resonator suitable for broadband materials characterisation, IET Microw., Antennas Propag. 2 (1) (2008) 66–73, https://doi.org/10.1049/iet-map:20070039.
[16] M. Boybay, O. Ramahi, Material characterization using complementary split-ring resonators, IEEE Trans. Instrum. Meas. 61 (2012) 3039, https://doi.org/10.1109/TIM.2012.2203450.
[17] A. Rashidian, M.T. Aligodarz, D.M. Klymyshyn, Dielectric characterization of materials using a modified microstrip ring resonator technique, IEEE Trans. Dielectr. Electr. Insul. 19 (4) (2012) 1392–1399, https://doi.org/10.1109/TDEI.2012.6260016.
[18] L. Yang, A. Rida, R. Vyas, M.M. Tentzeris, RFID tag and RF structures on a paper substrate using inkjet-printing Technology, IEEE Trans. Microw. Theor. Tech. 55 (12) (2007) 2894–2901, https://doi.org/10.1109/TMTT.2007.909886.
[19] "Aso-Oke Heritage, accessed, http://asooke.com.ng/www2/asooke.html#types, 2012. (Accessed 24 November 2020).
[20] O. Jide, A.B. Joseph, Aso-oke production and use among the Yoruba of southwestern Nigeria by, J. ofPan African Stud. 3 (3) (2009) 55–72.
[21] R.S. Kwok, J.-F. Liang, Characterization of high-Q resonators for microwave filter applications, IEEE Trans. Microw. Theor. Tech. 47 (1) (1999) 111–114, https://doi.org/10.1109/22.740093.